

# Active Linear Modeling of Cochlear Biomechanics Using Hspice

Soon Suck Jarng\*, You Jung Kwon\*

\*Dept. of Information, Control & Instrumentation, Chosun University, South Korea

(Received August 3 2005; revised Jun 6 2005; accepted September 8 2005)

## Abstract

This paper shows one and two dimensional active linear modeling of cochlear biomechanics using Hspice. The advantage of the Hspice modeling is that the cochlear biomechanics may be implemented into an analog IC chip. This paper explains in detail how to transform the physical cochlear biomechanics to the electrical circuit model and how to represent the circuit in Hspice code. There are some circuit design rules to make the Hspice code to be executed properly.

**Keywords:** Active, Linear, Cochlea, Biomechanics, Hspice, Modeling, Electric Circuit Model

## 1. Introduction

Since von Békésy first time experimentally analyzed the electrical functioning of the cochlea in 1938, not only physiological but also morphological researches have been done about the cochlea[1]. The measurement of the otoacoustic emission (OAE) by Kemp in 1970 promoted new approaches for the cochlear functioning research because he proved that the cochlea actively generated biological energy from inside the cochlea[2]. Last decades were tediously spent for searching the exact biomechanics of the cochlea. And one of the most significant results is that the outer hair cell (OHC) of the cochlea has the core role of the active biomechanics of the cochlea[3-5]. And the other important result is that the sharp frequency selectivity of the ear is mainly processed at the organ of corti rather than at the matrix of auditory nerves[6-8]. There are two important issues to be considered in the cochlear study; Frequency Selectivity, Intensity Sensitivity.

Frequency Selectivity: The frequency resolution of the ear is very fine. The frequency selectivity of the organ of corti is more

apparent at near the base than at the apex of the cochlea[9].

Intensity Sensitivity: The human ear shows about 120 dB dynamic range in sound intensity sensitivity[10]. The lowest sound pressure level of the hearing threshold is -10-0 dB SPL. The ear can endure some explosive high sound intensity such as 110-120 dB SPL for seconds. This wide dynamic range can be explained by the extraordinary biomechanics of the cochlea with not only nonlinear amplification but also nonlinear attenuation (suppression) abilities[11].

The most absolute method for the derivation of the cochlear biomechanics may be modeling of the cochlea. The more precisely tuned cochlear modeling would result in the more similar functioning of the cochlea in practice. The cochlear model has to pass the comparison process with experimentally measured results such as basilar membrane (BM) vibration, OAE, and two tone suppression etc.. The more advanced cochlear modeling includes the effect of the nonlinear force generation of the OHCs as well as the ion channeling of the hair cell stereocilia. Most of cochlear models are deductively made in imitation of the morphology of the organ of corti[12-14]. Also cochlear models can be inductively made from the experimental results such as frequency threshold curves (FTC). The former approach seems

Corresponding author: Soon Suck Jarng (ssjarng@chosun.ac.kr)  
Dept. of Information Control & Instrumentation, Chosun University,  
375 Seoseok-Dong, Donggo-Ku, Gwang-ju

not to be good enough to model for the wide dynamic range of the cochlea. The later method begins for example from an electrical active filter model such as sharp and narrow band pass (BP) filter, and then modifies the active filter parameters in order to get the similar results as the FTCs. The later method may be the alternative for the shortage of the former approach.

This paper shows one and two dimensional active linear modeling of cochlear biomechanics using Hspice[15]. The cochlear biomechanical modeling is based on the deductive approach as others but is processed using Hspice which is the most popular analog electric circuit simulator among electrical and electronic engineers. Because Hspice is so generally used for active filter design, the shortage of the present cochlear model may be supplemented with analog active filters added to the present model. This extra filtering may be arbitrary so as to be called as second filters. The advantage of the Hspice modeling is that the cochlear biomechanics may be implemented into an analog IC chip. This paper explains in detail how to transform the physical cochlear biomechanics to the electrical circuit model and how to represent the circuit in Hspice code.

## II. Methods

In physiological mechanisms, the mechanical vibrations impinging on the oval window of the cochlea are transmitted from the base to the apex through the cochlear fluid which causes the BM to vibrate at a characteristic place associated with the input acoustic wave frequency. Because adjacent places along the length of the BM vibrate in phase with the transmission of the fluid, the information of the phase as well as the amplitude of the BM displacement are both transmitted to the brain[16]. The cochlear biomechanics which include the phase processing of the vibrational signal can be modeled by a transmission line model of the cochlea[17-19]. The one-dimensional linear and active model of a cat suggested by Neely and Kim[12] was previously transformed to an electrical transmission line model by the author[20]. The electrical transmission line model was previously solved by the finite difference method (FDM). The same model is now extended to two dimensions and solved by Hspice in this paper.

The basic idea of Neely and Kim[12] for the cochlear biomechanics may be described as Fig. 1. Two masses coupled with four springs describe a simplified model of the segmented

cochlear partition. Both the BM and the tectorial membrane (TM) are attached at the spiral ligament and the spiral limbus respectively. This can be described as two masses attached at a reference ground by two damped springs. The OHC and the stereocilia connect the BM with the TM. This can be also described as the two masses coupled by two damped springs in series. This mechanical system of two masses with four springs results in the fourth order dynamic mechanics (Appendix 3). The active force generated by the OHC is transferred directly to the BM as well as indirectly to the TM through the stereocilia. The fourth order passive resonating system is actively tuned by the extra force. Neely and Kim suggested that the OHC generates the active force in proportion to the velocity of the OHC stereocilia [12].

The mechanical resonant system can be transformed to an electrical filter circuit by through/across analogy (Table 1). Mechanical variables such as force and velocity are analogies with current and voltage. Therefore the independent applied force and the dependent active force of the two masses - four springs system may be transformed to the independent current source,  $I_s$ , and the dependent current source,  $I_{OHC}$ , respectively (Fig. 2). Since the mechanical active force is in proportion to the velocity of the OHC stereocilia,  $I_{OHC}$  is depending upon the voltage across the stereocilia,  $V_{ST}$ . The actual value of  $I_{OHC}$  is

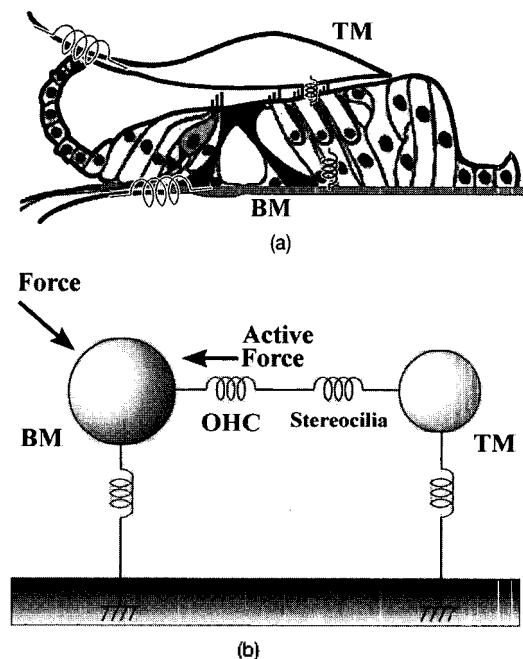


Fig. 1. (a) The cross section of the segmented cochlear partition, (b) Two masses coupled with four springs describe a simplified model of the cochlear biomechanics. BM: Basilar Membrane, TM: Tectorial membrane. The OHC and the stereocilia connect the BM with the TM.

Table 1. Mechanical / Electrical Analogies [21]

Analogy	Variables	Elements
Through/ Across	Force→Current Velocity→Voltage	Mass (M) ↔ Capacitance (C) Compliance (Cm) ↔ Inductance (L) Damping (Rm) ↔ Conductance (G)

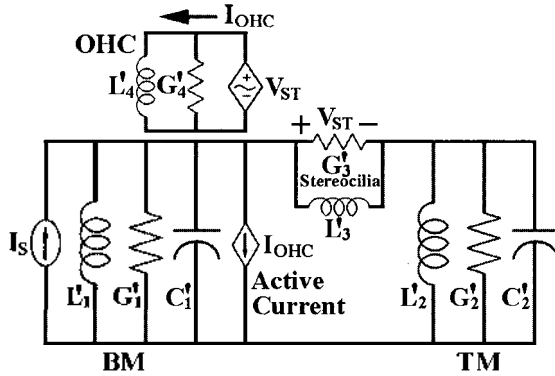


Fig. 2. The electrical through/across analogue of the two mass and four spring system.

the current passing through the OHC impedance,  $L'_4$  and  $G'_4$  where  $L'_4$  and  $G'_4$  are an electrical inductor and a conductor in analogy with the OHC mechanical compliance and damping.  $C'_1$ ,  $L'_1$  and  $G'_1$  are a capacitor, an inductor and a conductor in analogy with the BM mechanical mass, compliance and resistance

Table 2. Electrical Duality Principle [22]

Analogy	Variables	Elements
Force / Flow	Current ↔ Voltage	Capacitor (C) ↔ Inductor (L) Inductor (L) ↔ Capacitor (C) Conductor (G) ↔ Resistor (R)

Table 3. Mechanical / Electrical Analogies

Analogy	Variables	Elements
Force / Flow	Force→Voltage Velocity→Current  Applied Force→ $V_S$ Stereocilia Velocity→ $I_{ST}$ OHC Active Force→ $V_{OHC}$	Mass (M)→Inductance (L) Compliance (Cm)→Capacitance (C) Damping (Rm)→Resistance (R)  BM Mass→ $L_1$ BM Compliance→ $C_1$ BM Damping→ $R_1$ TM Mass→ $L_2$ TM Compliance→ $C_2$ TM Damping→ $R_2$ Stereocilia Compliance→ $C_3$ Stereocilia Damping→ $R_3$ OHC Compliance→ $C_4$ OHC Damping→ $R_4$

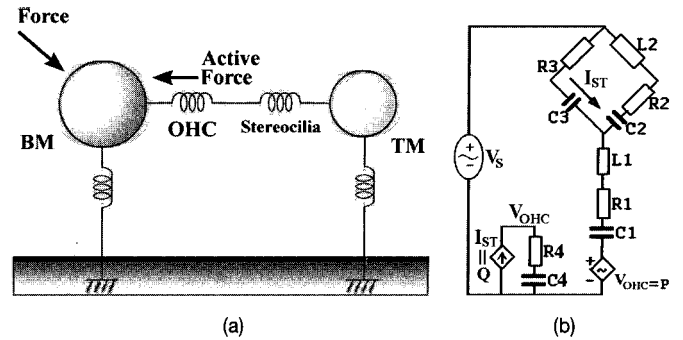


Fig. 3. (a) The cross section of the segmented cochlear partition, (b) The electrical force/flow analogue of the two mass and four spring system.  $I_{ST} \equiv Q$ ,  $V_{OHC} \equiv P$ .

respectively. In the same way,  $C'_2$ ,  $L'_2$  and  $G'_2$  are electric analogies of the TM elements, and  $L'_3$  and  $G'_3$  are electric analogies of the stereocilia elements

The electrical analogue of the two mass and four spring system is then converted from the through/across analogy to the force/flow analogy by the duality principle (Table 2). Figure 3 shows the result of the electrical duality principle applied to Fig.2.

Twice transformation of the two mass and three spring system result in the force/flow active filter circuit as shown in Fig. 3 which is more obvious physically than the through/across active filter circuit as shown in Fig. 2. Fig. 3 shows the impedance of the segmented cochlear partition.

The two dimensional transmission line model of the cochlea is shown in Fig. 4. The longitudinal length of a cat's cochlea is 2.5cm. The number of sections in the longitudinal direction, x-axis, from the base to the apex is 251 and those in the latitudinal direction, z-axis, is 11. Each of the longitudinal section of the first latitudinal layer represents the sectional impedance of the organ of corti (Fig. 3(b)). And the latitudinal layers throughout the whole longitudinal sections represent the fluid of the cochlea. The cochlear fluid is assumed to be incompressible and inviscid, so that the cochlear fluid is transformed and is modeled as a 11 by 251 rectangular matrix shape composed of 0.5 mH inductors. However very small  $20\mu\Omega$  resistors are added in series to the fluid inductor in the vertical direction but not in the horizontal direction. Those fluid resistors are added only for proper Hspice execution because Hspice can not solve the loop-like inductor circuit without some artificial addition of extra passive component such as resistor. The effects of the added small fluid resistors are negligible. The fluid resistor is not necessary in the horizontal direction. This is the first trick of the cochlear modeling and simulation using Hspice. If the latitudinal

sections are increased, the value of the fluid inductor becomes provisionally smaller. The last longitudinal section after the 251th section represents the helicotrema and is modeled as one single inductor of 2 mH.

The total electric circuit components are connected via nodes of which the number is not superimposed. The independent voltage source  $V_0$  is analogy with the sound pressure onto the ear drum. If we apply 0 dB SPL sound pressure onto the ear drum and the transfer gain between the ear drum and the stapes may be 70 [12], the peak-to-peak source voltage would be  $V_0(t) = [70 \cdot \sqrt{2} \cdot 2E-4] \cos(\omega \cdot t)$  [V].  $\omega$  is a angular frequency and  $t$  is a time variable [sec]. The passive impedance components (Lm[H], Rm[Ω], Cm[F]) represent the middle ear impedances, Zm; inductor(mass), resistor(damping), and capacitor(compliance) respectively (Appendix 1). LF is cochlear fluid inductance.

Fig. 5 shows the organ of corti longitudinally divided into impedance sections. Each impedance section is modeled as electric components such as resistor (R), inductor (L), capacitor (C) and dependant voltage source (P). Each sectional impedance,  $Z_i(x)$ , as a function of  $x$  is described in detail in Fig. 5, and their quantitative values are derived from the Neely and Kim's model (see Appendix 1). I and J represent electric loop currents in each section. Subscript number  $i$  indicates section numbers. The current which flows through the sectional stereocilia impedance, that is  $(I_{i-1}(t)-I_i(t))$ , represents the velocity of the OHC stereocilia at its corresponding point. The current dependant voltage,  $P_i(t)$ , represents the active force of the OHC, and it is proportional to the velocity of the stereocilia,  $I_{i-1}(t)-I_i(t)$ , as

follows;

$$P_i(t) = \gamma \cdot R4_i \cdot (I_{i-1}(t) - J_i(t)) - \frac{\gamma}{C4_i} \int (I_{i-1}(\tau) - J_i(\tau)) d\tau$$

$R4_i$  and  $C4_i$  represent characteristic impedances of the OHC.  $\gamma$  is an amplifying gain constant and the default value of  $\gamma$  is 1.0 for the present study. If  $\gamma$  is increased, the model becomes unstable, while smaller  $\gamma$  produces less sensitivity of the BM displacement [12, 20]. The spatial tuning resolution of the BM displacement for different  $\gamma$  is well published by Neely and Kim [12].

When the Fig. 5 circuit diagram is coded for Hspice execution, the circuit needs to be modified for proper Hspice execution as shown in Fig. 6. Three more tricks are added to the present model. The second trick is to add very big  $10^{18}\Omega$  resistors in parallel with  $C1_i$  capacitors. Those parallel resistors do not affect the simulation results but they make Hspice to execute properly. The third trick is to add  $1\Omega$  resistors in series with  $C3_i$  capacitors. Also those serial resistors do not affect the simulation results but they are added in order to produce voltage dependant current source,  $Q_i$ , in Hspice because Hspice does not execute for current dependant current source in the present circuit model. The third trick is to design current dependant voltage sources. That is to add  $1\Omega$  resistors in series with  $C3_i$  capacitors. Then the voltage dependant current source,  $Q_i$ , is in fact the same as current dependant current source because the voltage and the current are the same at the  $1\Omega$  resistor. Then R4 and C4 produce voltage across them because of  $Q_i$ . The forth trick is to make  $P_i$  as the voltage dependant voltage source.  $P_i$  produces

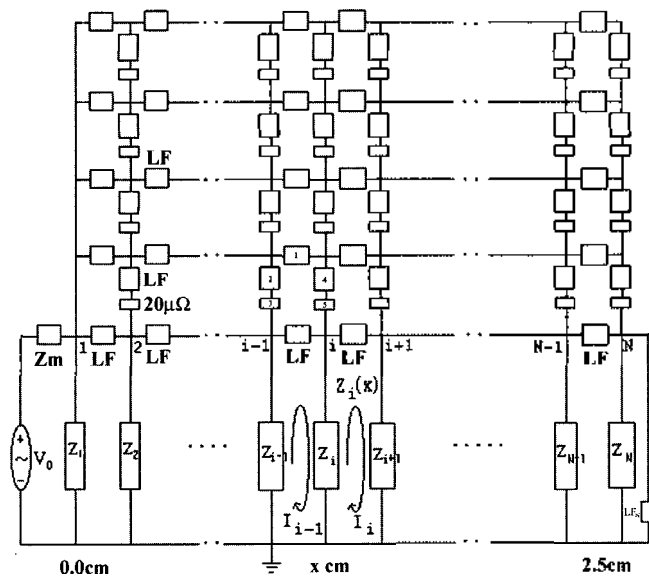


Fig. 4. Two dimensional transmission line model of the cochlea. N=250, LF=0.5 mH, LFN=2mH

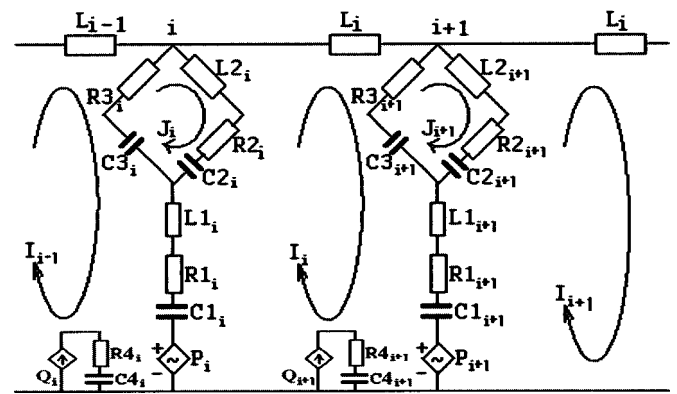


Fig. 5. The organ of corti is longitudinally divided into sections and each section is modeled as electric components such as resistor (R), inductor (L), capacitor (C) and current dependant voltage source (P) [20].

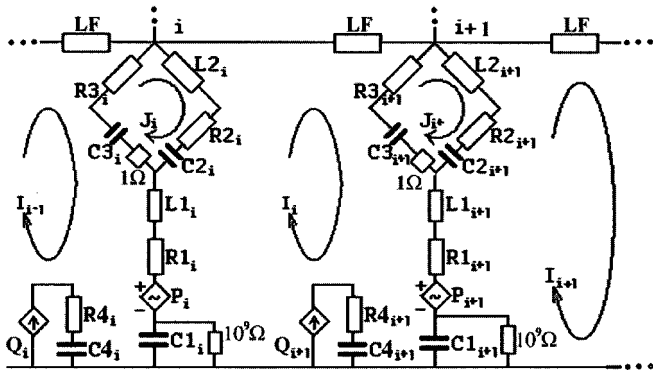


Fig. 6. Hspice version of each sectional impedance,  $Z_i(x)$

dependant voltage as proportional to the voltage across R4 and C4. We can change the amplifying gain constant,  $\gamma$ , by changing of the proportional constant of  $Q_i$ .

### III. Results and Discussion

Hspice codes of the cochlear model are written at Appendix 2. Hspice program was executed at SUN10 Unix workstation. Fig. 7 shows the simulation results of the one dimensional cochlear

model. The input frequency is 5 kHz and the amplification gain ( $\gamma$ ) is 1.0. Cochlear fluid mass, LF, is  $5E-3$  [H]. Fig. 7 (a) shows the displacement amplitude response of the basilar membrane vibration. X-axis is the distance from the base to the apex [cm]. Y-axis is the displacement magnitude in decibel scale with reference of nanometer  $10^{-9}$ [m]. The magnitude has its peak at about 0.92 [cm] and it has about 80 dB sharp tuning bandpass filter shape. The figure shows some slight fluctuation just before the sharp increase of the peak and the magnitude decreases very rapidly after the peak. If the amplification gain is increased the figure becomes sharper but it produces more fluctuation at the base side. This fluctuation means the backward transmit of the actively amplified biomechanical energy from the peak to the base. Therefore the amplification gain should be adjusted not to produce the fluctuation.

Fig. 7 (b) shows the displacement phase response of the basilar membrane vibration. The phase is unwrapped with respect of the distance. The total phase shift from the base to the apex is about  $24\pi$  [radians]. The pattern of the phase response may be divided into three parts; the slow slope from the base to about 0.75 [cm] position where the phase is slightly reversed, the rapid slope

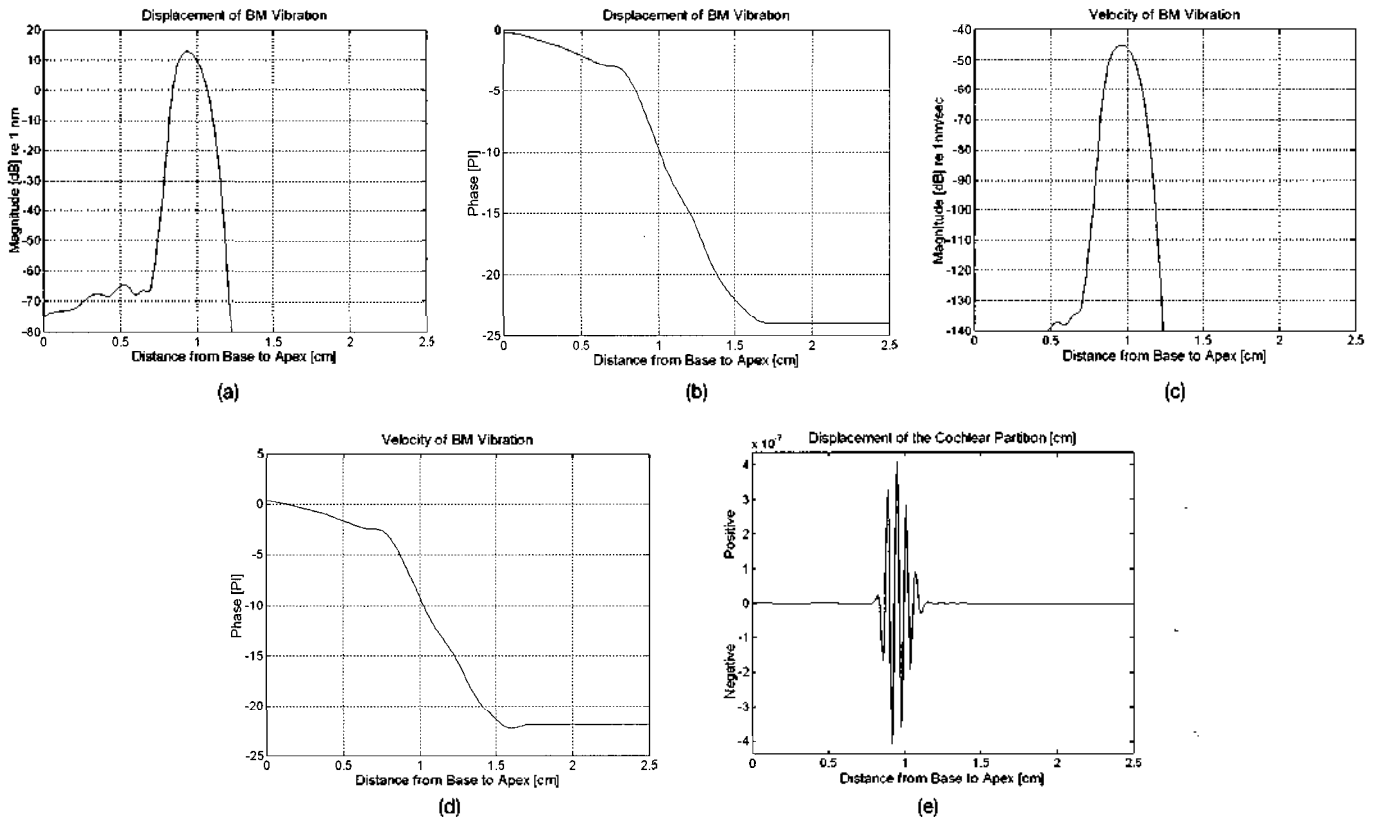


Fig. 7. (a) One dimensional cochlear model displacement amplitude response, (b) Displacement Phase response, (c) One dimensional cochlear model velocity amplitude response, (d) Velocity phase response, (e) Displacement time response, Input frequency = 5 kHz, Amplification Gain ( $\gamma$ )= 1, LF= $5E-3$  [H].

from about 0.75 [cm] position to about 1.7 [cm] position, the saddled slope after about 1.7 [cm] position. Fig. 7 (c) and Fig. 7 (d) are the velocity amplitude and phase responses of the basilar membrane vibration respectively. The velocity magnitude is in decibel scale with reference of  $10^{-9}$ [m/sec]. The magnitude has its peak at about 0.92 [cm] and it has about 95 dB sharp tuning bandpass filter shape. Fig. 7 (e) is the displacement temporal response of the basilar membrane vibration. Y-axis scale is linear. The  $24\pi$  [radians] phase shift around about 0.92 [cm] position significantly shows 5 cycles of vibrations which are physically unreasonable. Therefore the one dimensional cochlear model is not good enough for the simulation of the cochlear biomechanics.

Fig. 8 the simulation results of the two dimensional cochlear model. The input frequency is 5 kHz and the amplification gain ( $\gamma$ ) is 1.0. Cochlear fluid mass, LF, is  $5E-4$  [H]. Fig. 8 (a) shows the displacement amplitude response of the basilar membrane vibration. The magnitude has its peak at about 1.0 [cm] and it has about 30 dB sharp tuning bandpass filter shape. The figure shows no fluctuation just before the sharp increase of the peak and the magnitude does not decrease very rapidly after the peak. If the amplification gain is increased the bandpass filter shape becomes sharper. It should be noticed that there is an

amplitude notch just before the sharp increase of the peak. This notch may indicate the prohibition of the backward transmit of the actively amplified biomechanical energy from the peak to the base. Fig. 8 (b) shows the displacement phase response of the basilar membrane vibration. The total phase shift from the base to the apex is about  $3.5\pi$  [radians]. One significant pattern of the phase response is that the phase is reversed at about 0.75 [cm] position where the amplitude rapidly increases. Fig. 8 (c) and Fig. 8 (d) are the velocity amplitude and phase responses of the basilar membrane vibration respectively. And Fig. 8 (e) is the displacement temporal response of the basilar membrane vibration. The  $3.5\pi$  [radians] phase shift around about 1.0 [cm] position significantly shows 2 cycles of vibrations which are physically reasonable. Therefore the two dimensional cochlear model looks better than the one dimensional simulation of the cochlear biomechanics.

Fig. 9 shows the simulation results of the two dimensional cochlear model with different frequencies; 6400 [Hz], 1600 [Hz], 400 [Hz]. The amplification gain ( $\gamma$ ) is 1.0. Cochlear fluid mass, LF, is  $5E-3$  [H]. Fig. 9 (a) and Fig. 9 (b) are the displacement amplitude and phase responses respectively. As the input frequency decreases, the peak moves toward the apex. The

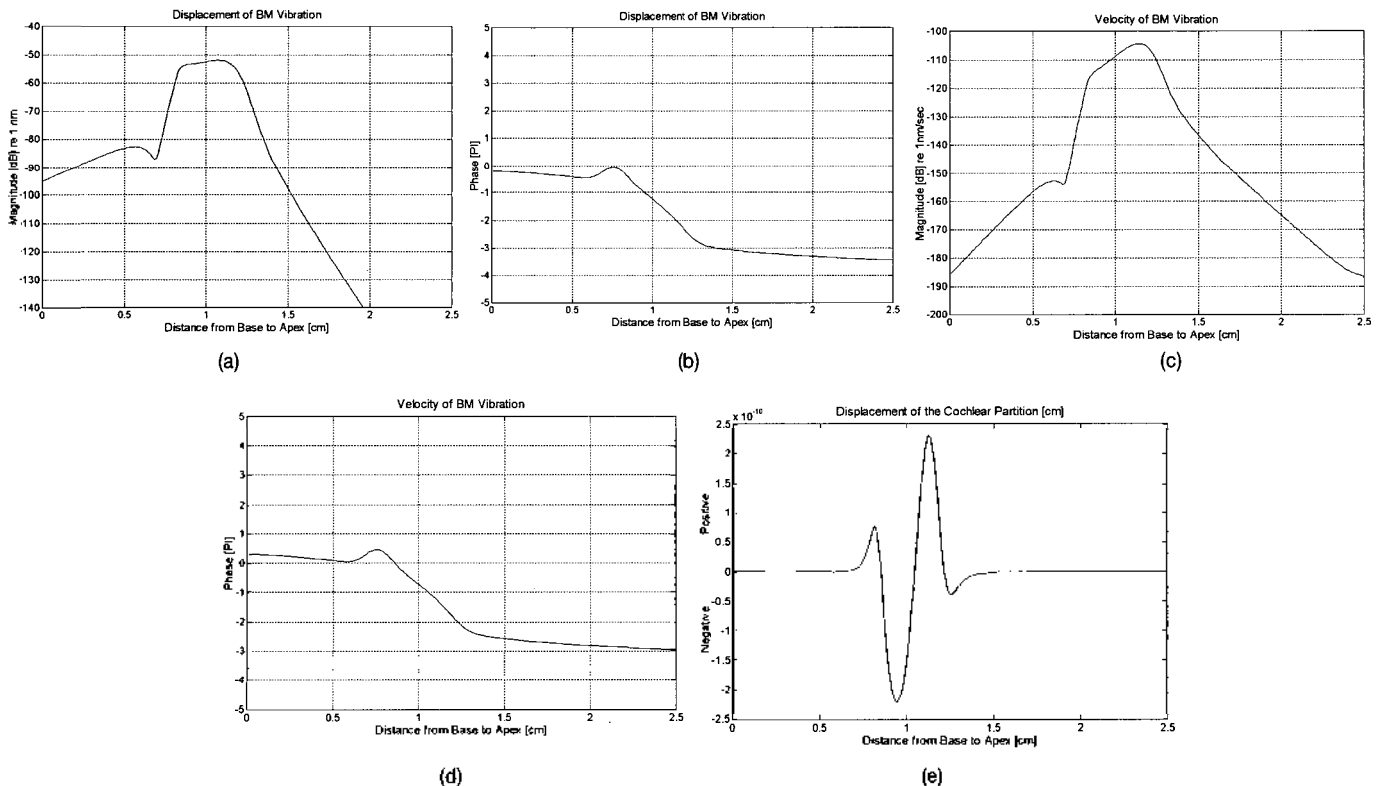


Fig. 8. (a) Two dimensional cochlear model displacement amplitude response, (b) Displacement Phase response, (c) Two dimensional cochlear model velocity amplitude response, (d) Velocity phase response, (e) Displacement time response. Input frequency = 5 kHz, Amplification Gain ( $\gamma$ )= 1, LF= $5E-4$  [H].

increase of the cochlear fluid mass not only increases the sharpness of the bandpass filter shape but also increases the amount of the phase shift. The increase of the sharpness is more significant than the increase of the phase shift. Fig. 9 (c), Fig. 9 (d) and Fig. 9 (e) show the displacement temporal responses of the basilar membrane vibration at each different input frequency respectively.

#### IV. Conclusion

This paper shows one and two dimensional active linear modeling of cochlear biomechanics using Hspice. The advantage of the Hspice modeling is that the cochlear biomechanics may be implemented into an analog IC chip. This paper explains in detail how to transform the physical cochlear biomechanics to the electrical circuit model and how to represent the circuit in Hspice code. There are some circuit design rules to make the Hspice code to be executed properly.

#### Appendix 1 Notification of Symbols

- $\theta$  = phase [radian]
- $f$  = frequency [Hz]
- $t$  = time [sec]
- $x$  = distance from the base [cm]
- $\omega$  = angular frequency ( $= 2\pi f$ )
- $P_i(t)$  = dependant voltage [V]
- $Z_i(x)$  = section impedance of the transmission line
- $N$  = section impedance of the transmission line ( $= 251$ )
- $\gamma$  = active amplifying gain=1.0
- $dx$  = distance between two adjacent sections =  $1E-2$  [cm]
- $V_o(t)$  = input voltage source equivalent to sound pressure onto the ear drum [v]
- $R_m$  = middle ear characteristic resistance =  $400$  [ $\Omega$ ]
- $L_m$  = middle ear characteristic inductance =  $4.5E-2$  [ $H$ ]
- $C_m$  = middle ear characteristic capacitance =  $4.762E-6$  [ $F$ ]
- $LF_N$  = cochlear fluid inductance =  $2E-3$  [ $H$ ]
- $LF$  = cochlear fluid inductance (1D) =  $5E-3$  [ $H$ ]

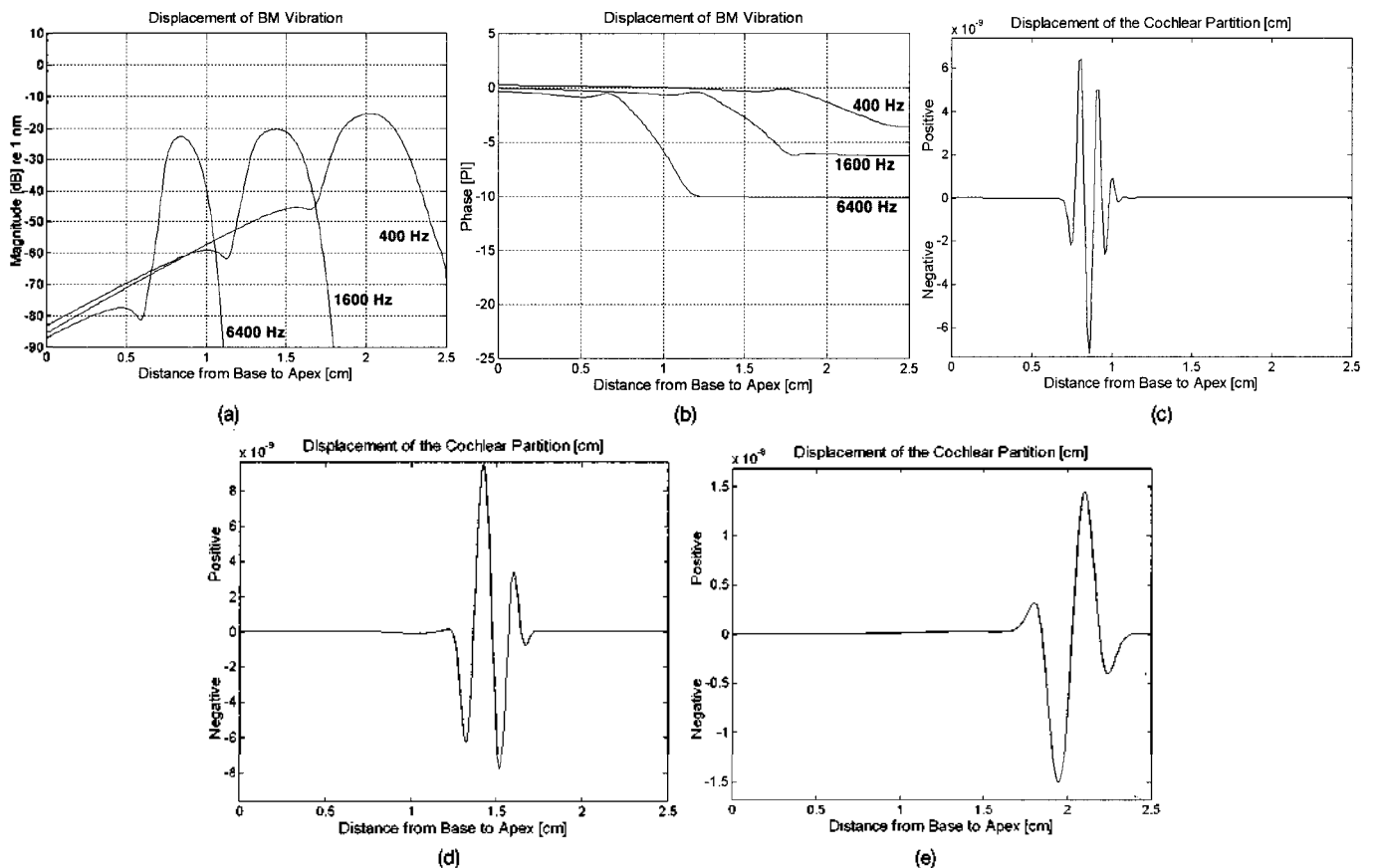


Fig. 9. (a) Two dimensional cochlear model displacement amplitude responses, (b) Displacement Phase responses, (c) Displacement time response (6400 Hz), (d) Displacement time response (1600 Hz), (e) Displacement time response (400 Hz). Amplification Gain ( $\gamma$ )= 1,  $LF=3E-3$  [ $H$ ].

$LF = \text{cochlear fluid inductance (2D)} = 5E-4 [H]$   
 $R_1(x) = \text{BM characteristic resistance} = 20.0 + 1500.0 \times \exp(-2.0 \cdot x)$   
 $[\Omega]$   
 $L_1(x) = \text{BM characteristic inductance} = 3.0E-3 [H]$   
 $C_1(x) = \text{BM characteristic capacitance} = 0.9091E-9 \times \exp(4.0 \cdot x)$   
 $[F]$   
 $R_2(x) = \text{TM characteristic resistance} = 10.0 \times \exp(-2.2 \cdot x) [\Omega]$   
 $L_2(x) = \text{TM characteristic inductance} = 0.5E-3 \times \exp(x) [H]$   
 $C_2(x) = \text{TM characteristic capacitance} = 1.429E-7 \times \exp(4.4 \cdot x) [F]$   
 $R_3(x) = \text{OHC Stereocilia characteristic resistance} = 2.0 \times \exp(-0.8 \cdot x)$   
 $[\Omega]$   
 $C_3(x) = \text{OHC Stereocilia characteristic capacitance} =$   
 $1.0E-7 \times \exp(4.0 \cdot x) [F]$   
 $R_4(x) = \text{OHC characteristic resistance} = 1040.0 \times \exp(-2.0 \cdot x) [\Omega]$   
 $C_4(x) = \text{OHC characteristic capacitance} = 1.626E-9 \times \exp(4.0 \cdot x)$   
 $[F]$

#### Appendix 2 Hspice code of the cochlear model

##### 251 CASECADED SPICE MODEL OF THE BM

```

VIN 1 0 AC 0.0198 0.0
LM 1 2 4.500000e-002
RM 2 3 4.000000e+002
CM 3 4 4.762000e-006
RCM 3 4 1.000000e+009
LF1 4 15 5.000000e-004
R31 4 5 2.000000e+000
C31 5 14 1.000000e-007
R_C1 14 6 1.000000e+000
L21 4 7 5.000000e-004
R21 7 8 1.000000e+001
C21 8 6 1.429000e-007
L11 6 9 3.000000e-003
R11 9 10 1.520000e+003
ECCS1 10 11 12 0 -1.000000e+000
C11 11 0 9.091000e-010
R51 11 0 1.000000e+018
GCCS1 0 12 14 6 1.000000e+000
R41 12 13 1.040000e+003
C41 13 0 1.626000e-009
LF2 15 26 5.000000e-004
.
.
.
LF251 2754 0 2.000000e-003
R3251 2754 2755 2.728359e-001
C3251 2755 2764 2.116617e-003
R_C251 2764 2756 1.000000e+000
L2251 2754 2757 6.030878e-003
R2251 2757 2758 4.177311e-002
C2251 2758 2756 8.189148e-003

```

```

L1251 2756 2759 3.000000e-003
R1251 2759 2760 3.031027e+001
ECCS251 2760 2761 2762 0 -1.000000e+000
C1251 2761 0 1.924216e-005
R5251 2761 0 1.000000e+018
GCCS251 0 2762 2764 2756 1.000000e+000
R4251 2762 2763 7.148455e+000
C4251 2763 0 3.441619e-005
LHF21 4 3015 5.000000e-004
LHF22 3015 3016 5.000000e-004
LVF22 3015 2765 5.000000e-004
RVF22 2765 15 2.000000e-005
LHF23 3016 3017 5.000000e-004
LVF23 3016 2766 5.000000e-004
RVF23 2766 26 2.000000e-005
LHF24 3017 3018 5.000000e-004
LVF24 3017 2767 5.000000e-004
RVF24 2767 37 2.000000e-005
LHF25 3018 3019 5.000000e-004
LVF25 3018 2768 5.000000e-004
RVF25 2768 48 2.000000e-005
LHF26 3019 3020 5.000000e-004
LVF26 3019 2769 5.000000e-004
RVF26 2769 59 2.000000e-005
LHF27 3020 3021 5.000000e-004
LVF27 3020 2770 5.000000e-004
RVF27 2770 70 2.000000e-005
LHF28 3021 3022 5.000000e-004
LVF28 3021 2771 5.000000e-004
RVF28 2771 81 2.000000e-005
LHF29 3022 3023 5.000000e-004
LVF29 3022 2772 5.000000e-004
RVF29 2772 92 2.000000e-005
.
.
.
LHF11248 7761 7762 5.000000e-004
LVF11248 7761 7511 5.000000e-004
RVF11248 7511 7261 2.000000e-005
LHF11249 7762 7763 5.000000e-004
LVF11249 7762 7512 5.000000e-004
RVF11249 7512 7262 2.000000e-005
LHF11250 7763 7764 5.000000e-004
LVF11250 7763 7513 5.000000e-004
RVF11250 7513 7263 2.000000e-005
LVF11251 7764 7514 5.000000e-004
RVF11251 7514 7264 2.000000e-005
.AC LIN 1 5000 5000
.PRINT AC VM(11) VP(11)
.PRINT AC VM(22) VP(22)
.
.
.PRINT AC VM(2750) VP(2750)
.PRINT AC VM(2761) VP(2761)
.END

```



Appendix 3 The fourth order dynamic mechanics of the cochlear partition impedance

$$Z_1 = R_1 + L_1 \cdot S + \frac{1}{C_1 \cdot S} \quad (A3.1)$$

$$Z_2 = R_2 + L_2 \cdot S + \frac{1}{C_2 \cdot S} \quad (A3.2)$$

$$Z_3 = R_3 + \frac{1}{C_3 \cdot S} \quad (A3.3)$$

$$Z_4 = R_4 + \frac{1}{C_4 \cdot S} \quad (A3.4)$$

$$V_S = V_x + Z_1 \cdot I_1 + V_{OHC} \quad (A3.5)$$

$$V_x = I_{ST} \cdot Z_3 = (I_1 - I_{ST}) \cdot Z_2 \quad (A3.6)$$

$$\text{From (A3.6)} \quad I_1 = \frac{Z_2 + Z_3}{Z_2} \cdot I_{ST} \quad (A3.7)$$

$$V_{OHC} = \gamma \cdot V_4 \quad (A3.8)$$

$$V_4 = Z_4 \cdot I_{ST} \quad (A3.9)$$

$$\text{From (A3.8) and (A3.9)} \quad V_{OHC} = \gamma \cdot Z_4 \cdot I_{ST} \quad (A3.10)$$

$$V_{out} = I_1 \cdot \frac{1}{C_1 \cdot S} \quad (A3.11)$$

$$\text{From (A3.7) and (A3.10)} \quad I_{ST} = \frac{Z_2}{Z_2 + Z_3} \cdot I_1 = \frac{Z_2 \cdot C_1 \cdot S}{Z_2 + Z_3} \cdot V_{out} \quad (A3.12)$$

From (A3.5), (A3.6), (A3.11) and (A3.10)

$$V_S = \frac{Z_3 \cdot Z_2 \cdot C_1 \cdot S}{Z_2 + Z_3} \cdot V_{out} + Z_1 \cdot C_1 \cdot S \cdot V_{out} + \gamma \cdot \frac{Z_4 \cdot Z_2 \cdot C_1 \cdot S}{Z_2 + Z_3} \cdot V_{out} \quad (A3.13)$$

$$\text{Therefore} \quad H(S) = \frac{1}{\frac{Z_3 \cdot Z_2 \cdot C_1 \cdot S}{Z_2 + Z_3} + Z_1 \cdot C_1 \cdot S + \gamma \cdot \frac{Z_4 \cdot Z_2 \cdot C_1 \cdot S}{Z_2 + Z_3}} \quad (A3.14)$$

## Acknowledgment

This study was supported by IDEC (KAIST Integrated Design Education Center) semiconductor design tool 2005

## References

1. von Békésy G, *Experiments in hearing*, (Wiley, New York, 1960.)
2. Kemp D.T., "Stimulated acoustic emissions from within the human auditory system", *J. Neurophysiology*, **34**, 802-816, 1978.
3. Ashmore J.F., "A fast motile response in guinea-pig outer hair cells: the molecular basis of the cochlear amplifier", *J. of Physiology*

(London), **388**, 323-347, 1987.

4. Iwasa K.H. and Chadwick R.S., "Elasticity and active force generation of cochlear outer hair cells", *J. Acoust. Soc. Am.*, **92** (6), 3169-3173, 1992.
5. Dallos P., "Cochlear neurobiology", *The cochlea*, Edited by P. Dallos, A.N. Popper, and R.R. Fay, New York, Springer, 186-257, 1996.
6. Sellick P.M., Patuzzi R., Johnstone B.M., "Measurement of basilar membrane motion in the guinea pig using the Mössbauer technique", *J. Acoust. Soc. Am.*, **72**, 131-141, 1982.
7. Khanna S.M., Leonard D.G.B., "Basilar membrane tuning in the cat cochlea", *Science*, **215**, 305-306, 1982.
8. Narayan S.S., Temchin A.N., Recio A., and Ruggero M.A., "Frequency tuning of basilar membrane and auditory nerve fibers in the same cochleae", *Science*, **282**, 1882-1884, 1998.
9. Pickles J.O., *An introduction to the physiology of hearing*, (Academic Press, London and New York, 1982.)
10. Allen J.B., "Nonlinear cochlear signal processing", in Jahn, Anthony F. and Santos-Sacchi, Joseph, Eds. *Physiology of the Ear*, Second Edition, Singular Thompson, chapter 19, 393-442, 2001.
11. Rhode W.S., "Observations of the vibration of the basilar membrane in squirrel monkeys using the Mössbauer technique", *J. Acoust. Soc. Am.*, **49**, 1218-1231, 1971.
12. Neely S.T., Kim D.O., "A model for active elements in cochlear biomechanics", *J. Acoust. Soc. Am.*, **79**, 1472-1480, 1986.
13. Chadwick R.S., "Compression, gain, and nonlinear distortion in an active cochlear model with subpartitions", *Proc. Natl. Acad. Sci. USA*, **95**, 14594-14599, 1998.
14. Neely S.T., Gorga M.P. and Dorn P.A., "Growth of distortion-product otoacoustic emissions in a nonlinear, active model of cochlear mechanics", *Biophysics of the cochlea*, ed. By A.W.Gummer, World Scientific, 531-538, 2003.
15. Hspice User's Guide, 2002.
16. Evans E.F., Wilson J.P., *Psychophysics and physiology of hearing*, (Academic Press, London and New York), 5-54, 1977.
17. Wegel R.L. and Lane C.E., "The auditory masking of one pure tone by another and its probable relation to the dynamics of the inner ear", *Physical Review*, **23**, 266-285, 1924.
18. Schroeder M.R., "An integrable model for the basilar membrane", *J. Acoust. Soc. Am.*, **53** (1), 429-434, 1973.
19. Zwicker E., "A hardware cochlear nonlinear preprocessing model with active feedback", *J. Acoust. Soc. Am.*, **80** (1), 146-153, 1986.
20. Jang S.S., "Electrical transmission line modeling of the cochlear basilar membrane" *J. of Korea Soc. of Med. and Bio. Eng.*, **14** (2), 125-136, 1993.
21. Usher M.J., "Sensors and transducers", Macmillan, ISBN 0-333-38709-0, 1-20, 1985.
22. Alexander C.K and Sadiku M.N.O., *Fundamentals of Electric Circuits*, (McGRAW-HILL Korea), 422-426, 2001.

## [Profile]

•Soon Suck Jang



1984.2: Hanyang Uni. (S. Korea), Dept. of Electronics (B.Eng.)

1985.9: Hull Uni. (U.K.), Dept. of Electronics (M.Eng.)

1988.9: Birmingham Uni. (U.K.), Dept. of Physiology (M.Sc.)

1991.12: Birmingham Uni. (U.K.), Dept. of Electronic Electrical Eng. (Ph.D.)

1992.3.-Present Professor in the Dept. of Information Control & Instrumentation, Chosun University (South Korea)

※Main Research: Cochlear Bio-mechanics, Hearing Aids, Piezoelectric Sensor

Device, Finite Element Method (FEM), Boundary Element Method (BEM)

•You Jung Kwon



1987.2: Yonsei Uni. (S. Korea), Dept. of Food & Science (B.Sc.)

2005.2: Chosun Uni. (S. Korea), Dept. of Information Control & Instrumentation (M.Eng.)

2005.3~Present: Ph.D. student in the Dept. of Information Control & Instrumentation, Chosun University (S. Korea)

※Main Research: Cochlear Bio-mechanics, Hearing Aids